Journal of Nuclear Medicine, published on July 29, 2021 as doi:10.2967/jnumed.121.262045

First-in-human evaluation of a PD-L1-binding peptide radiotracer in non-small cell lung cancer patients with PET

*Xin Zhou[1, #], Jinquan Jiang[1, #], Xue Yang[2, #], Teli Liu[1], Jin Ding[1], Sridhar Nimmagadda[3], Martin G Pomper[3], Hua Zhu[1, *], Jun Zhao[2, *], Zhi Yang[1, *], Nan Li[1, *]*

[1]Key laboratory of Carcinogenesis and Translational Research (Ministry of Education/Beijing), Department of Nuclear Medicine, NMPA Key Laboratory for Research and Evaluation of Radiopharmaceuticals (National Medical Products Administration), Peking University Cancer Hospital & Institute, Beijing, 100142, China; [2]Key laboratory of Carcinogenesis and Translational Research (Ministry of Education/Beijing), Department I of Thoracic Oncology, Peking University Cancer Hospital & Institute, Beijing, 100142, China; [3]The Russell H. Morgan Department of Radiology and Radiological Science, Johns Hopkins University School of Medicine, Baltimore, Maryland, USA.

[#] These authors contributed equally to this work

[*] Correspondence

Corresponding authors:

Nan Li, No.52 Fucheng Rd., Beijing, 100142, China. E-mail: rainbow6283@sina.com, Tel./Fax: +86-10-88196196.

Zhi Yang, No.52 Fucheng Rd., Beijing, 100142, China. E-mail: pekyz@163.com, Tel./Fax: +86-10-88196196.

Jun Zhao, No.52 Fucheng Rd., Beijing, 100142, China. E-mail: ohjerry@163.com, Tel./Fax: +86-10-88196456.

Hua Zhu, No.52 Fucheng Rd., Beijing, 100142, China. E-mail: zhuhuananjing@163.com, Tel./Fax: +86-10-88196196.

First authors:

Xin Zhou (student), No.52 Fucheng Rd., Beijing, 100142, China. E-mail: zhouxinbjmu@163.com, Tel./Fax: +86-10-88196196.

Jinquan Jiang (student), No.52 Fucheng Rd., Beijing, 100142, China. E-mail: jiangjinquan1989@163.com, Tel./Fax: +86-10-88196196.

Xue Yang (resident), No.52 Fucheng Rd., Beijing, 100142, China. E-mail: dryangxue2010@163.com, Tel./Fax: +86-10-88196456.

Conflict of interest: The authors declare no potential conflicts of interest.

Financial support: National Science and Technology Major Project (No. 2020ZX09201023), National Natural Science Foundation of China (81671733, 81871386, and 81871387), Beijing Excellent Talents Funding (2017000021223ZK33).

Word count: 4874

Running title: PD-L1 targeted peptide-based radiotracer

ABSTRACT

Background: ^{68}Ga-NOTA-WL12 is a peptide-based positron emission tomography (PET) imaging agent. We conducted a first-in-human study of ^{68}Ga-NOTA-WL12 for PET to study the in vivo biodistribution, metabolism, radiation dosimetry, safety, and potential for quantifying programmed death ligand-1 (PD-L1) expression levels in advanced non-small cell lung cancer (NSCLC) patients. **Methods:** In vitro assessment of the PD-L1 expression and cellular uptake of ^{68}Ga-NOTA-WL12 were performed, followed by in vivo evaluation of ^{68}Ga-NOTA-WL12 uptake in mouse models with tumors. Nine NSCLC patients with lesions expressing PD-L1 were enrolled and monitored for adverse events during the study. ^{68}Ga-NOTA-WL12 and paired ^{18}F-FDG PET/CT imaging were performed. Uptake (SUV/L and kBq/mL) values of tumors and normal organs were obtained. Radiopharmaceutical biodistribution, radiation dosimetry and the relationship of tumor uptake to PD-L1 expression were evaluated. Follow-up ^{18}F-FDG PET/CT was performed in patients who had undergone treatment with a combination of pembrolizumab with chemotherapy. **Results:** ^{68}Ga-NOTA-WL12 exhibited PD-L1 specific uptake in vitro and in PD-L1-positive tumors in vivo. ^{68}Ga-NOTA-WL12 PET imaging proved safe with acceptable radiation dosimetry. Physiological tracer uptake was mainly visible in the liver, spleen, small intestine and kidney. Tumors were clearly visible, particularly in the lungs, with a T/lung ratio of 4.45 ±1.89 at 1 h. One hour was a suitable time-point for image acquisition because no significant differences were noted in tumor-to-background ratios

between 1 and 2 h. A strong, positive correlation was found between tumor uptake (SUV_{peak}) and PD-L1 immunohistochemistry results ($r = 0.9349$; $P = 0.002$). ^{68}Ga-NOTA-WL12 and ^{18}F-FDG PET studies suggest that PD-L1 PET before therapy may indicate the therapeutic efficacy of pembrolizumab plus chemotherapy combination treatment. **Conclusions:** Our first-in-human findings demonstrate the safety and feasibility of ^{68}Ga-NOTA-WL12 for noninvasive, in vivo detection of tumor PD-L1 expression levels, indicating potential benefits for clinical PD-L1 therapy.

Key words: PD-(L)1, PET/CT, immune checkpoint inhibitor, non-small cell lung cancer, Pembrolizumab

INTRODUCTION

Treatment of non-small cell lung cancer (NSCLC) has advanced considerably over the past 40 years. In addition to the advent of molecularly targeted therapies, inhibition of immune checkpoints using anti-programmed cell death (ligand)-1 [PD-(L)1] monoclonal antibodies has revolutionized the management of patients with advanced NSCLC(*1-6*).

Therapeutics targeting the PD(L)-1 axis are now a first-line option for advanced NSCLC without genetic aberrations(*7*). Numerous clinical studies have shown that PD-L1 expression identified NSCLC patients who are most likely to respond to immunotherapy, such as pembrolizumab(*7,8*). FDA-approved PD-L1 assessment using immunohistochemistry and its interpretation is often based on a single biopsy or several small biopsies, which poorly represent the heterogeneity of PD-L1 expression within and between patients(*9,10*). Additionally, tumor biopsy is not always practical when the lesion site is inaccessible. These limitations indicate a need for tools to detect PD-L1 levels in the whole body to improve our understanding of the response of NSCLC to therapies targeting the PD(L)-1 axis.

Positron emission tomography (PET) enables quantitative, real-time, non-invasive assessment of target expression levels and dynamics in the whole body(*11,12*). Recently, several studies have investigated molecular imaging of PD-L1 expression. Biologics, such as radiolabeled antibodies and adnectin-derived small protein radiotracers, have shown promise in early phase clinical trials(*13-18*). High-affinity, low-molecular-weight radiotracers labeled with ^{64}Cu, ^{68}Ga, and ^{18}F have been developed and shown to detect

graded levels of PD-L1 expression in vivo in preclinical models of several cancer types, including NSCLC(*13-15*,*19*,*20*). One of those agents, WL12, is a high-affinity PD-L1-binding small peptide labeled with ^{68}Ga. ^{68}Ga-WL12 proved a suitable scaffold for imaging PD-L1 expression in preclinical studies with PET(*19*). The tractable pharmacokinetics and high contrast PD-L1-specific images exhibited by ^{68}Ga-WL12 within 60 min of injection indicate the potential for further evaluation and clinical translation. Here, we report the first-in-human evaluation of a peptide-based PET imaging agent derived from WL12, ^{68}Ga-NOTA-WL12 (Supplemental Figure 1A), as well as its safety, radiation dosimetry and imaging characteristics, to compare PET imaging with immunohistochemistry and therapy evaluation in patients with advanced NSCLC.

MATERIALS AND METHODS

General

This is a prospective, phase I, open-label, nonrandomized, diagnostic imaging study in advanced NSCLC patients (n=9) between March 2020 and September 2020 (Trial registration ID: NCT04304066). Medical Ethics Committee of Peking University Cancer Hospital (2019 KT62) approved this study. Oral and written informed consent was obtained from all the participants.

NOTA-WL12 was custom synthesized and provided by Chinapeptides (Shanghai, China). Briefly, to radiolabel NOTA-WL12, 925~1110 Mbq $^{68}GaCl_3$ was mixed with 195 μL 1 *M* (pH 8.5) sodium acetate buffer and reacted with NOTA-WL12 (30 μg) at 60℃ for 15 min. The final product was sep-pak purified and obtained in > 99% radiochemical purity

by HPLC. Details regarding the production, quality control and murine radiotoxicity of ^{68}Ga-NOTA-WL12 can be found in the Supplemental Materials (Supplemental Table 1).

The patients inclusion criteria are: (1) clinical diagnosed NSCLC patients with positive PD-L1 expressing; (2) Eastern Cooperative Oncology Group performance score of 0-2. Exclusion criteria: (1) severe liver or kidney dysfunction; (2) chemoradiotherapy or targeted therapy before PET/CT scans. PD-L1 expression in available lesions was evaluated by immunohistochemistry using antibody clone 22C3 (Dako Denmark A/S; catalog M3653). Dako PD-L1 immunohistochemistry 22C3 pharmDx is an approved screening criterion for pembrolizumab application in NSCLC(*21*,*22*). Positive PD-L1 expression was defined as a tumor proportion score (TPS) ≥ 1%, while high PD-L1 expression was defined as a TPS ≥ 50%.

Flow Cytometric Analysis and Small-animal PET

Chinese hamster ovary (CHO) cell line was obtained from American Type Culture Collection (Manassas, Virginia, USA). CHO cell line with constitutive PD-L1 expression (CHO-hPD-L1) was generated in our laboratory and described previously(*23*). Details of the cell culture, flow cytometry analysis for PD-L1 expression, and in vitro assays are provided in the Supplemental Materials.

For PET imaging, NOD/SCID mice bearing CHO-hPD-L1 or CHO tumors were intravenously injected with ~7.4 MBq (~0.17μg) of ^{68}Ga-NOTA-WL12 in 200 μL of saline and PET images were acquired at 30, 60 and 120 min. To establish in vivo specificity, animals were co-injected with 50 μg of unlabeled WL12. Image analysis and PD-L1 IHC of the CHO-hPD-L1 and CHO tumors tumors are described in the Supplemental Materials.

PET/CT

Patients were injected intravenously with ^{68}Ga-NOTA-WL12 (1.9-3.7 MBq/kg). To determine the optimal peptide dose required to obtain high-contrast images, an escalated non-radiolabeled WL12 mass dose was co-administered with the imaging agent. The first two patients received 0 μg, the next 3 received 5 ug, then 60 ug, and the final group of 3 received 120 μg. Because patients co-administered with 120 μg of WL12 showed lower uptake in the liver, the last 4 patients were co-injected with 120 μg of WL12. The first patient underwent a dynamic scan at six time points in 1 h. The remaining eight patients underwent PET/CT 1 h after injection, and six of those were also scanned 2 h after injection (two patients were unable to tolerate the full 2 h examination). Imaging was performed using a Biograph mCT Flow 64 scanner (Siemens, Erlangen, Germany) [120 kV; 146 mAs; slice: 3 mm; matrix: 200 × 200; iterations:2; subsets: 11; filter: 5 mm Gaussian], continuously moving the patient bed at a speed of 1.5 mm/s to cover the entire body, from the top of the skull to the middle of the femur. Images were reconstructed with ordered

subset expectation maximization. CT reconstruction used a standard method with a 512 × 512 matrix and a layer thickness of 3–5 mm. CT data were used to correct the PET images for attenuation. Vital signs, laboratory studies and electrocardiograms were obtained before injection, during the screening period, and 2 days after PET/CT. All patients underwent paired ^{18}F-FDG PET/CT scans (1 h after injection) within a week after ^{68}Ga-NOTA-WL12 PET/CT using the same imaging system. Three patients repeated the ^{18}F-FDG PET/CT examination within 3 weeks after combination therapy including pembrolizumab and chemotherapy.

Radiation Dosimetry

Data from four patients with 120 μg of co-injected WL12 was used for ^{68}Ga-NOTA-WL12 dosimetry analysis, and the heart contents, lungs, liver, spleen, pancreas, kidneys, uterus, urinary bladder contents and body remainder were selected as source organs. The volumes of the source organs manually drawn on CT images were calculated, and their mean counts/mL (kBq/mL) were determined from PET images at 1 and 2h timepoints. Dosimetry was estimated using OLINDA/EXM software (version 2.0; Hermes Medical Solutions AB). Detailed procedures are provided in the Supplemental Materials.

Image Analysis

Image analysis was performed by two experienced nuclear medicine physicians. The uptake parameters of major organs, tissues and lesions were obtained to determine the organ biodistribution. SUV lean (SUL) was obtained by standardizing SUV to the body mass, which is less dependent on body habitus(*24*). No significant difference was observed in the coefficients of variation between SUL_{mean} and SUV_{mean} (Supplemental Figure 2A and Supplemental Table 2). Accordingly, we used SUL_{mean} and percentage (%) of injected activity to describe radiopharmaceutical uptake in normal organs. To compare the uptake differences between the liver, spleen, small intestine (SI) and kidney among patients co-administered with different doses of WL12, multi-site measurement was applied and the uptake was calculated as an average of the number of patients corresponding to different dose administrations separately (Supplemental Figure 3). To analyze normal organ uptake at different time-points, six patients with 1- and 2-h imaging were involved. The maximum, peak and mean values of SUV/L in biopsied lesions were obtained and were used to correlate with PD-L1 tumor proportion score (TPS). Tumor uptake of ^{68}Ga-NOTA-WL12 higher than that of blood pool (BP) was considered positive. Evaluation of the therapeutic response was based on PET Response Criteria in Solid Tumors(*24*) (PERCIST, for ^{18}F-FDG PET/CT evaluations) and Response Evaluation Criteria in Solid Tumors(*25*) (RECIST 1.1, for CT evaluations) standards.

Statistics

Differences and correlations among parameters were tested using the Wilcoxon signed-rank test, Mann–Whitney U test, and Spearman correlation using IBM SPSS Statistics (version 24; IBM Corp.) software. *P*-values < 0.05 were considered statistically significant.

RESULTS

Safety Assessment

^{68}Ga-NOTA-WL12 was produced with > 99% purity with a specific activity of 18.5–296 GBq/μmol (Supplemental Figure 1B). The safety parameters were measured. Murine radiotoxicity indicated that 167-200 MBq ^{68}Ga-NOTA-WL12 was safe for human being (Supplemental Figure 4). Details can be found in the Supplemental Materials.

In Vitro Cellular Studies and Small-Animal PET Imaging

Flow cytometry showed that the mean fluorescence intensity values of CHO-hPD-L1 was higher than CHO, so was cellular uptake extent (Supplemental Figure 5).

NOD/SCID mice bearing CHO-hPD-L1 tumors showed intense uptake of ^{68}Ga-NOTA-WL12 in the tumors by 120 min (T/BP: 4.5 ± 0.2; T/M: 19.1 ± 1.2) (Figure 1), while negative control CHO tumors showed minimal uptake (Supplemental Figure 6A).

Additionally, tumor uptake decreased with the co-injection of NOTA-WL12, indicating in vivo specificity (Figure 2). Immunohistochemistry analysis showed high PD-L1 expression in CHO-hPD-L1 tumors (Supplemental Figure 6B).

Patient Characteristics

Nine patients (8 men and 1 woman; median age, 68 y; range, 47-80 y) with histopathologically proven NSCLC (5 adenocarcinoma, 4 squamous cell carcinoma) were included. Clinical stage, therapeutic regimen, PD-L1 expression and other characteristics are summarized in Table 1. The mean administered radioactivity of ^{68}Ga-NOTA-WL12 was 195 ± 30 MBq (range, 167–270 MBq).

Safety

Nine ^{68}Ga-NOTA-WL12 PET/CT examinations were performed, with no adverse or clinically detectable pharmacologic effects. No significant changes were observed in vital signs, results of laboratory studies or electrocardiograms.

Biodistribution

Uptake of ^{68}Ga-NOTA-WL12 was mainly observed in the SI and liver, followed by moderate-to-low uptake in the kidneys, tumor and spleen, and low uptake in the lungs and bone marrow (Figure 3). This uptake pattern was similar to that observed in preclinical

studies(*19,20,26,27*). With an increasing precursor dose co-administered with ^{68}Ga-NOTA-WL12, we observed decreased and increased uptake in the liver and SI, respectively, as well as a gradual decrease in the spleen uptake. Radioactivity uptake in the kidneys and blood pool at 1h remained similar irrespective of the mass of WL12 used (Figure 3; Supplemental Figure 7A, B). Uptake observed in the liver, small intestine and kidneys indicates that clearance of ^{68}Ga-NOTA-WL12 was primarily through the hepatobiliary system and secondarily through renal excretion. Except for the significant increase in uptake in SI and the significant decrease in uptake in the liver from 1 h to 2 h, other normal organs showed a downward trend with no significant differences (Supplemental Figure 7C, D).

Radiation Dosimetry

Table 2 summarizes the individual organ doses and effective doses of patients administered ^{68}Ga-NOTA-WL12 with120 μg of WL12 (n=4) [administered dose: 224 ± 37 (range, 192–270 MBq)]. The SI (3.47E-01 mGy/MBq) received the highest dose, indicating that WL12 is metabolized by hepatobiliary clearance, a characteristic observed with lipophilic agents. The intestinal absorbed dose remained well below the threshold for the human intestinal acute dose (6 Gy)(*28*). Radiation dosimetry was acceptable at 1.85E-02 ± 4.07E-03 mSv/MBq (4.1 mSv per patient), which is lower than the radiation dose of conventional ^{18}F-FDG PET/CT (7.0–14 mSv)(*29*).

Tumor Uptake and Correlation with Immunohistochemistry

Rapid clearance of radioactivity was observed from the blood pool (BP), resulting in high tumor-to-BP (and muscle) ratios. Thus, the T/BP and T/muscle ratios were 1.48 ± 0.42 and 1.56 ±0.49 and 5.31 ± 1.99 and 4.87 ±1.28 at 1 h and 2 h, respectively. High contrast was also observed in the lungs with T/lung ratios of 4.45 ± 1.89 and 5.18 ± 2.27 at 1 h and 2 h, respectively. No significant differences were noted in the tumor-to-background ratios (BP, lungs, and M) at 1 and 2 h (Supplemental Figure 2B), indicating that 1 h after radiotracer administration is a suitable time-point for image acquisition.

In patients with high PD-L1 expression, tumor uptake of ^{68}Ga-NOTA-WL12 (TPS: 80%; SUV_{max}: 4.87) was higher than that of patients with low PD-L1 expression (TPS: 8%; SUV_{max}: 1.84) (Figure 4). All calculated PET parameters of ^{68}Ga-NOTA-WL12, except for the ratios of tumor uptake to BP, correlated with the corresponding PD-L1 TPS on immunohistochemistry (Supplemental Table 3) [SUV_{peak} (r_s= 0.9349, P = 0.002) (Figure 5A)]. In contrast to ^{68}Ga-NOTA-WL12, uptake of ^{18}F-FDG in the lesions did not correlate with PD-L1 expression, with a tenuous relationship to SUV_{mean} (r_s = 0.6937; P = 0.0382) (Figure 5B).

We also noted the intra- and inter-tumoral heterogeneity of ^{68}Ga-NOTA-WL12 uptake in some patients, reflecting the heterogeneity of PD-L1 expression reported with other PD-L1 imaging agents(*13,16*) (Figure 6). The uptake of ^{18}F-FDG was intense in the tumors

regardless of PD-L1 expression levels, with no significant heterogeneity among or within lesions.

Relationship of ^{68}Ga-NOTA-WL12 Uptake to Therapy

Three subjects underwent ^{18}F-FDG PET/CT after combination (pembrolizumab plus chemotherapy) treatment. In subjects #1 and #6, with PD-L1 TPS values of 8% and 30%, respectively, ^{68}Ga-NOTA-WL12 uptake in tumors before treatment showed SUV_{max} values of 2.21 and 3.05 (Figure 7, A, B; Supplemental Table 4), respectively. These two subjects were rated as partial metabolic responses [PMR, PERCIST(*24*)] and stable disease [SD, RECIST 1.1(*25*)].

Subject #3, with a PD-L1 TPS value of 8%, showed negative ^{68}Ga-NOTA-WL12 uptake before therapy (SUV_{max} of tumor: 1.84; SUV_{max} of BP: 1.78). This patient showed increased uptake of ^{18}F-FDG in the primary tumor and a new brain metastasis on the post-therapy scan, and he was further rated as progressive disease (PD, PERCIST and RECIST) (Figure 7, C and Supplemental Table 4). Thus, subjects with PMR/SD exhibited positive uptake of ^{68}Ga-NOTA-WL12 before therapy.

DISCUSSION

We describe the first-in-human evaluation of ^{68}Ga-NOTA-WL12, a peptide-based PD-L1 imaging agent, in patients with NSCLC. We demonstrated that ^{68}Ga-NOTA-WL12 is safe and effective for PET imaging of PD-L1 expression.

Inhibition of the PD(L)-1 axis has proved a remarkable success in treating patients with NSCLC(*1-4*). PD-L1 expression, determined by needle biopsy, is currently the only validated biomarker used as a companion diagnostic test for NSCLC patient selection for pembrolizumab therapy(*22*). Several studies have demonstrated variations in PD-L1 expression within patients and within tumors, due to heterogeneity of target expression(*30*). PD-L1 heterogeneity may still confound a single positive biopsy result, leading to inappropriate administration of therapy, contributing to the moderate correlation between PD-L1 status and survival rates(*30*). However, nuances in PD-L1 heterogeneity and its relevance to response are emerging. Patients with PD-L1 TPS values ≥ 50% can now be treated with pembrolizumab as a first-line option, indicating that increased PD-L1 expression is related to improved clinical outcomes(*31*). Patients with PD-L1 expression > 75% and > 90% have benefitted more than those with 50%-75%, suggesting that analysis and correlation of outcome data using PD-L1 expression on a continuous 0%-100% scale rather than using predefined cutoffs (≥ 50%) would be more accurate. These studies indicate that PD-L1 heterogeneity is an underappreciated aspect in assessing and guiding immune checkpoint therapies. Furthermore, these issues are compounded in advanced-

stage NSCLC patients because a biopsy of every lesion is not feasible. Noninvasive quantification of PD-L1 levels could provide complementary information to address those challenges, as shown herein and by other groups(*13,16*).

Many radiolabeled probes targeting PD-L1 have been validated in preclinical models, such as antibodies, antibody fragments, small proteins and peptides(*13-17*). Correspondingly, the preclinical experiments in this study confirmed that the uptake of ^{68}Ga-NOTA-WL12 was highly correlated to PD-L1 expression. The accumulation of ^{89}Zr-atezolizumab, a PD-L1 antibody, in patients with breast, lung and bladder cancers showed a higher predictive value than immunohistochemistry or genomic sequencing for therapeutic response(*16*). Additionally, the accumulation of ^{89}Zr-atezolizumab and another PD-L1 PET imaging agent, ^{18}F-BMS-986192, was found to be heterogeneous between and within patients(*13,16*). Several studies revealed that the addition of non-radiolabeled peptide precursor reduced liver uptake through competitive metabolism; however, the excretion of ^{68}Ga-NOTA-WL12 to the SI was elevated with the increase in the peptide dose. That finding differed from other saturation antibody studies(*32*), suggesting that the mass of ^{68}Ga-NOTA-WL12 in circulation was relatively stable, and the addition of peptide would not likely affect tumor uptake. Therefore, patients who different mass doses of peptide precursor were enrolled. The correlation between uptake and therapeutic outcome, together with the inter- and intra-tumor heterogeneity observed with ^{68}Ga-NOTA-WL12 uptake, indicated the potential to predict immune-therapy.

Radiolabeled antibodies such as ^{89}Zr-atezolizumab and ^{89}Zr-nivolumab, because of their long physical half-life and circulation times, may encounter difficulties in delineating the changes in PD-L1 expression(*13*,*16*). Additionally, PET measures of radiolabeled antibodies do not accurately measure target expression; they are a combination of tracer exposure and target expression(*16*). Small-molecule radiotracers such as ^{68}Ga-NOTA-WL12 provide a direct measure of the PD-L1 status within hours of radiotracer administration, likely because of better tissue penetration. Characteristics WL12 peptide binding to PD-L1 also present opportunities to quantify the pharmacologic activity of PD-L1 antibodies within the tumor bed in a manner agnostic to the antibody type, as recently shown in preclinical models(*20*).

Therapeutic evaluation based on ^{18}F-FDG PET/CT for lung cancer is widely recognized by physicians(*24*,*33*). Three patients in this study who received immunotherapy underwent ^{18}F-FDG PET/CT for therapeutic evaluation. Patients with positive uptake of ^{68}Ga-NOTA-WL12 were rated as having a PMR, and patients with a negative uptake of ^{68}Ga-NOTA-WL12 were rated as having PD. Although two of the three patients shared the same PD-L1 expression level (TPS: 8%), the outcomes (PMR and PD) were quite different. These results suggest that higher ^{68}Ga-NOTA-WL12 uptake in lesions may indicate a better prognosis than lower ^{68}Ga-NOTA-WL12 uptake, regardless of the level of PD-L1 expression determined by immunohistochemistry. Those observations in a small number of patients merit further validation in larger patient cohorts.

A potential limitation of our study is the small number of patients involved. Nonetheless, our study is similar to other first-in-human phase 1 studies of radiopharmaceuticals, and has sufficient power to assess safety, suitable imaging time-points, radiation dosimetry, and preliminary correlation of ^{68}Ga-NOTA-WL12 uptake with immunohistochemistry. Another limitation of the study is that immunohistochemistry was performed only on index lesions, limiting our ability to quantify intra-lesional variation within a given patient.

CONCLUSION

This first-in-human study of ^{68}Ga-NOTA-WL12, a low-molecular-weight peptide-derived imaging agent, demonstrates the feasibility and potential of quantifying PD-L1 levels in NSCLC with PET within a clinically viable time-frame. ^{68}Ga-NOTA-WL12 proved safe with favorable biodistribution and radiation dose estimates, similar to those of other radiopharmaceuticals. ^{68}Ga-NOTA-WL12 uptake measures correlated with PD-L1 levels detected by immunohistochemistry, suggesting its suitability as a complementary diagnostic to immunohistochemistry to quantify PD-L1 levels for patient selection and therapeutic monitoring in anti-PD-L1 therapy.

Acknowledgments:

S.N. and M.G. P were not directly involved with the data acquisition but contributed to the interpretation of the acquired data and preparation of the manuscript. S. N and M.G. P are supported by NIH 1R01CA236616 and NIH P41EB024495. S.N. and M.G.P. are co-inventors on a pending U.S. patents covering WL12 and, as such, are entitled to a portion of any licensing fees and royalties generated by this technology. This arrangement has been reviewed and approved by Johns Hopkins University in accordance with its conflict-of-interest policies. S. N and M.G.P. are consultants for Precision Molecular Inc., which has licensed the patent covering WL12 from Johns Hopkins University, and own equity in D&D Pharmatech, the parent company of Precision Molecular, Inc.

Key Points:

Question:

Can the peptide-based radiotracer ^{68}Ga-NOTA-WL12 detect and represent the expression levels of PD-L1 in patients with NSCLC?

Pertinent Findings:

We demonstrated the feasibility and potential of ^{68}Ga-NOTA-WL12 to quantify PD-L1 levels in preclinical models and in patients with NSCLC, with a strong relationship between tumor uptake and PD-L1 immunohistochemistry.

Implications for Patient Care:

^{68}Ga-NOTA-WL12 can be used to image PD-L1 in vivo, indicating its potential as a complementary diagnostic to immunohistochemistry to quantify PD-L1 levels for patient selection and therapeutic monitoring in anti-PD-L1 therapy.

REFERENCES:

1. Rittmeyer A, Barlesi F, Waterkamp D, et al. Atezolizumab versus docetaxel in patients with previously treated non-small-cell lung cancer (OAK): a phase 3, open-label, multicentre randomised controlled trial. *Lancet*. 2017;389:255-265.

2. Brahmer J, Reckamp KL, Baas P, et al. Nivolumab versus docetaxel in advanced squamous-cell non-small-cell lung cancer. *N Engl J Med*. 2015;373:123-135.

3. Borghaei H, Paz-Ares L, Horn L, et al. Nivolumab versus docetaxel in advanced nonsquamous non-small-cell lung cancer. *N Engl J Med*. 2015;373:1627-1639.

4. Gandhi L, Rodríguez-Abreu D, Gadgeel S, et al. Pembrolizumab plus Chemotherapy in Metastatic Non-Small-Cell Lung Cancer. *N Engl J Med*. 2018;378:2078-2092.

5. Antonia SJ, Borghaei H, Ramalingam SS, et al. Four-year survival with nivolumab in patients with previously treated advanced non-small-cell lung cancer: a pooled analysis. *Lancet Oncol*. 2019;20:1395-1408.

6. Remon J, Passiglia F, Ahn MJ, et al. Immune Checkpoint Inhibitors in Thoracic Malignancies: Review of the Existing Evidence by an IASLC Expert Panel and Recommendations. *J Thorac Oncol*. 2020;15:914-947.

7. Rosner S, Reuss JE, Forde PM. PD-1 Blockade in Early-Stage Lung Cancer. *Annu Rev Med*. 2019;70:425-435.

8. Mok TSK, Wu Y-L, Kudaba I, et al. Pembrolizumab versus chemotherapy for previously untreated, PD-L1-expressing, locally advanced or metastatic non-small-cell lung cancer (KEYNOTE-042): a randomised, open-label, controlled, phase 3 trial. *Lancet*. 2019;393:1819-1830.

9. Kluger HM, Zito CR, Turcu G, et al. PD-L1 studies across tumor types, its differential expression and predictive value in patients treated with immune checkpoint inhibitors. *Clin Cancer Res*. 2017;23:4270-4279.

10. McLaughlin J, Han G, Schalper KA, et al. Quantitative assessment of the heterogeneity of PD-L1 expression in non-small-cell lung cancer. *JAMA Oncol*. 2016;2:46-54.

11. Willmann JK, van Bruggen N, Dinkelborg LM, Gambhir SS. Molecular imaging in drug development. *Nat Rev Drug Discov*. 2008;7:591-607.

12. Kobayashi H, Longmire MR, Ogawa M, Choyke PL, Kawamoto S. Multiplexed imaging in cancer diagnosis: applications and future advances. *Lancet Oncol*. 2010;11:589-595.

13. Niemeijer AN, Leung D, Huisman MC, et al. Whole body PD-1 and PD-L1 positron emission tomography in patients with non-small-cell lung cancer. *Nat Commun*. 2018;9:4664.

14. Xing Y, Chand G, Liu C, et al. Early phase I study of a ^{99m}Tc-labeled anti-programmed death ligand-1 (PD-L1) single-domain antibody in SPECT/CT assessment of PD-L1 expression in non-small cell lung cancer. J *Nucl Med*. 2019;60:1213-1220.

15. Donnelly DJ, Smith RA, Morin P, et al. Synthesis and biologic evaluation of a novel ^{18}F-labeled adnectin as a PET radioligand for imaging PD-L1 expression. *J Nucl Med*. 2018;59:529-535.

16. Bensch F, van der Veen EL, Lub-de Hooge MN, et al. ^{89}Zr-atezolizumab imaging as a non-invasive approach to assess clinical response to PD-L1 blockade in cancer. *Nat Med*. 2018;24:1852-1858.

17. Heskamp S, Hobo W, Molkenboer-Kuenen JD, et al. Noninvasive imaging of tumor PD-L1 expression using rdiolabeled anti-PD-L1 antibodies. *Cancer Res*. 2015;75:2928-2936.

18. Huisman MC, Niemeijer AN, Windhorst AD, et al. Quantification of PD-L1 expression with ^{18}F-BMS-986192 PET/CT in patients with advanced-stage non-small cell lung cancer. *J Nucl Med*. 2020;61:1455-1460.

19. De Silva RA, Kumar D, Lisok A, et al. Peptide-based ^{68}Ga-PET radiotracer for imaging PD-L1 expression in cancer. *Mol Pharm*. 2018;15:3946-3952.

20. Kumar D, Lisok A, Dahmane E, et al. Peptide-based PET quantifies target engagement of PD-L1 therapeutics. *J Clin Invest*. 2019;129:616-630.

21. U.S. Food and Drug Administration. Dako PD-L1 IHC 22C3 pharmDx. September 2015: http://www.accessdata. fda.gov/cdrh_docs/pdf15/P150013c.pdf. Accessed 10 August 2016.

22. Herbst RS, Baas P, Kim D-W, et al. Pembrolizumab versus docetaxel for previously treated, PD-L1-positive, advanced non-small-cell lung cancer (KEYNOTE-010): a randomised controlled trial. *Lancet*. 2016;387:1540-1550.

23. Chatterjee S, Lesniak WG, Gabrielson M, et al. A humanized antibody for imaging immune checkpoint ligand PD-L1 expression in tumors. *Oncotarget*. 2016;7:10215-10227.

24. Wahl RL, Jacene H, Kasamon Y, Lodge MA. From RECIST to PERCIST: Evolving considerations for PET response criteria in solid tumors. *J Nucl Med*. 2009;50 Suppl 1:122S-150S.

25. Eisenhauer EA, Therasse P, Bogaerts J, et al. New response evaluation criteria in solid tumours: revised RECIST guideline (version 1.1). *Eur J Cancer*. 2009;45:228-247.

26. Lesniak WG, Mease RC, Chatterjee S, et al. Development of [(18)F]FPy-WL12 as a PD-L1 specific PET imaging peptide. *Mol Imaging*. 2019;18:1536012119852189.

27. Chatterjee S, Lesniak WG, Miller MS, et al. Rapid PD-L1 detection in tumors with PET using a highly specific peptide. *Biochem Biophys Res Commun*. 2017;483:258-263.

28. FA S, AV A, M H-J, et al. ICRP publication 118: ICRP statement on tissue reactions and early and late effects. *Ann ICRP 2012*; 41(1-2):1-322 - 1-322.

29. Delbeke D, Coleman RE, Guiberteau MJ, et al. Procedure guideline for tumor imaging with ^{18}F-FDG PET/CT 1.0. *J Nucl Med*. 2006;47:885-895.

30. Hofman P. PD-L1 immunohistochemistry for non-small cell lung carcinoma: which strategy should be adopted? *Expert Rev Mol Diagn*. 2017;17:1097-1108.

31. Aguilar EJ, Ricciuti B, Gainor JF, et al. Outcomes to first-line pembrolizumab in patients with non-small-cell lung cancer and very high PD-L1 expression. *Ann Oncol*. 2019;30:1653-1659.

32. Sörensen J, Velikyan I, Sandberg D, et al. Measuring HER2-Receptor Expression In Metastatic Breast Cancer Using [68Ga]ABY-025 Affibody PET/CT. *Theranostics*. 2016;6:262-271.

33. Beer L, Hochmair M, Haug AR, et al. Comparison of RECIST, iRECIST, and PERCIST for the Evaluation of Response to PD-1/PD-L1 Blockade Therapy in Patients With Non-Small Cell Lung Cancer. *Clin Nucl Med*. 2019;44:535-543.

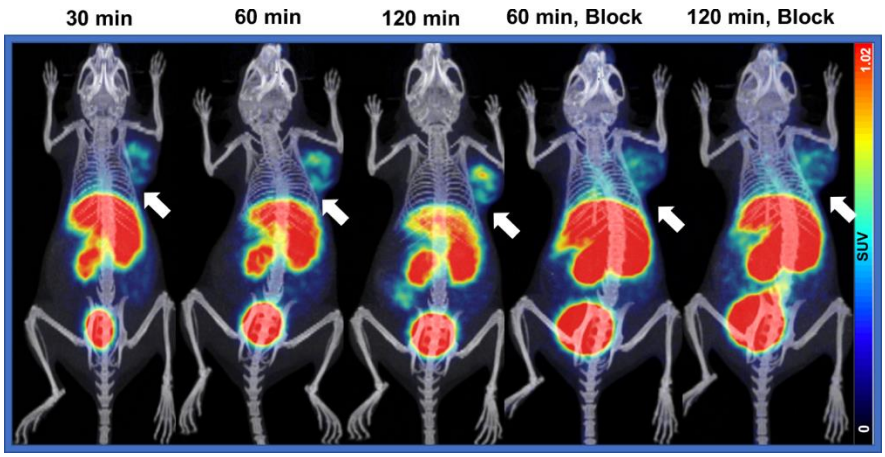

Figure 1. PET/CT images of NOD/SCID mice with CHO-hPD-L1 tumors at different time points after ^{68}Ga-NOTA-WL12 injection and of mice receiving 50 µg amount of blocking dose.

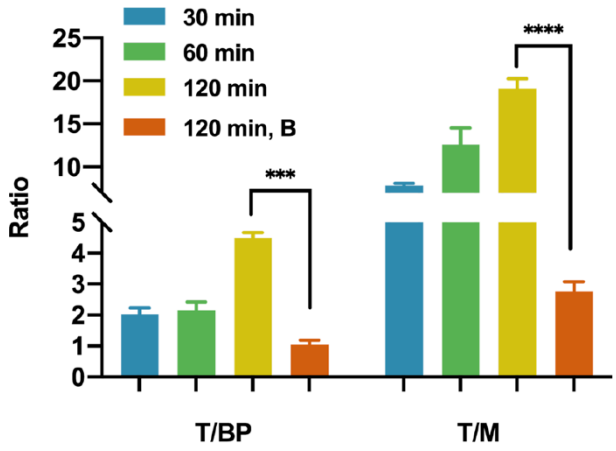

Figure 2. Ratios of tumor-to-blood-pool uptake (T/BP) and tumor-to-muscle uptake (T/M) in mice receiving ^{68}Ga-NOTA-WL12 with and without blocking dose at different time points.

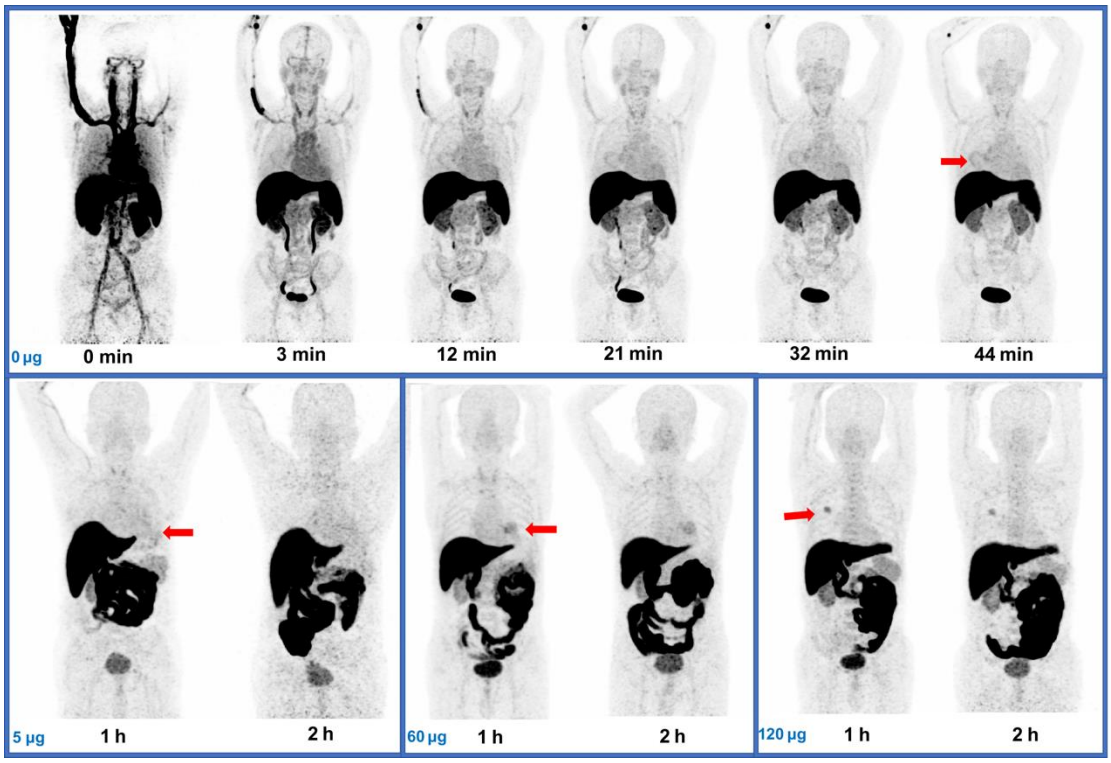

Figure 3. Maximum intensity projection imaging for biodistribution and organ uptake of ^{68}Ga-NOTA-WL12 at different time points after injection administered without and with increasing precursor doses (5 μg, 60 μg, 120 μg). Primary lesions are indicated by red arrows.

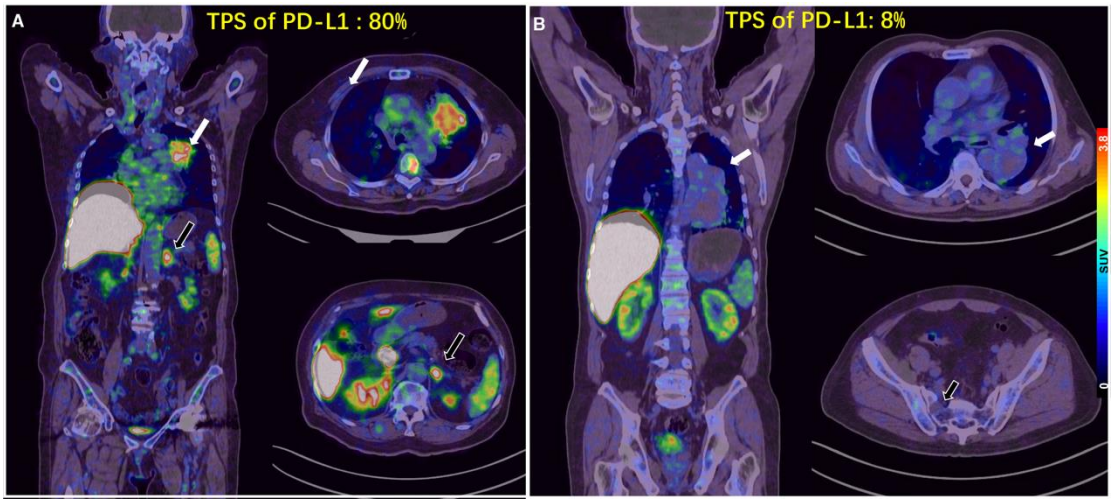

Figure 4. A, Patient 9, an 80-year-old woman with advanced NSCLC and a PD-L1TPS of 80%. The SUV_{max} of the primary tumor was 4.87 (white arrow), and that of left adrenal metastasis was 5.47 (black arrow) on ^{68}Ga-NOTA-WL12 PET. B, Patient 3, a 68-year-old man with a PD-L1 TPS of 8%. The SUV_{max} values of the primary tumor in the left lung and right sacral metastasis were 1.84 and 0.8, respectively, on ^{68}Ga-NOTA-WL12 PET.

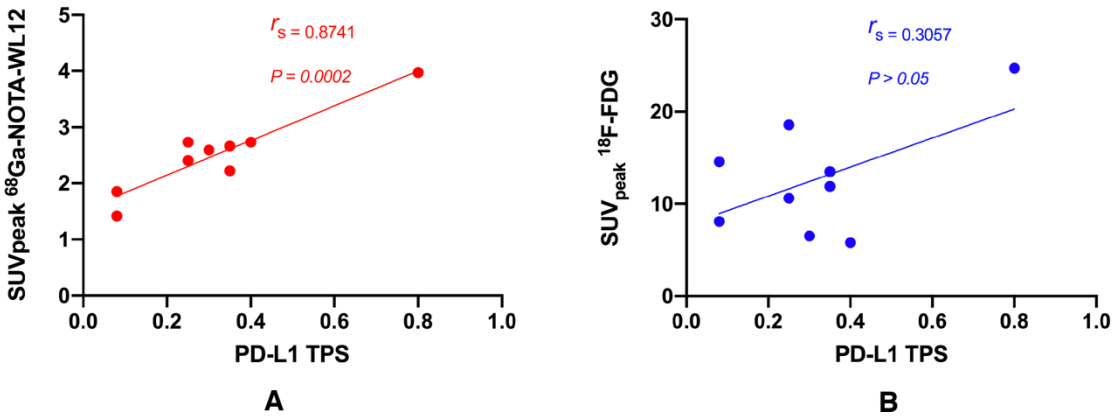

Figure 5. Relationship between PD-L1 expression detected by immunohistochemistry and tumor uptake (SUV_{peak}) of [^{68}Ga]NOTA-WL12 (r_s=0.8741, p<0.0005) (A) and ^{18}F-FDG (r_s=0.3057, P>0.05) (B).

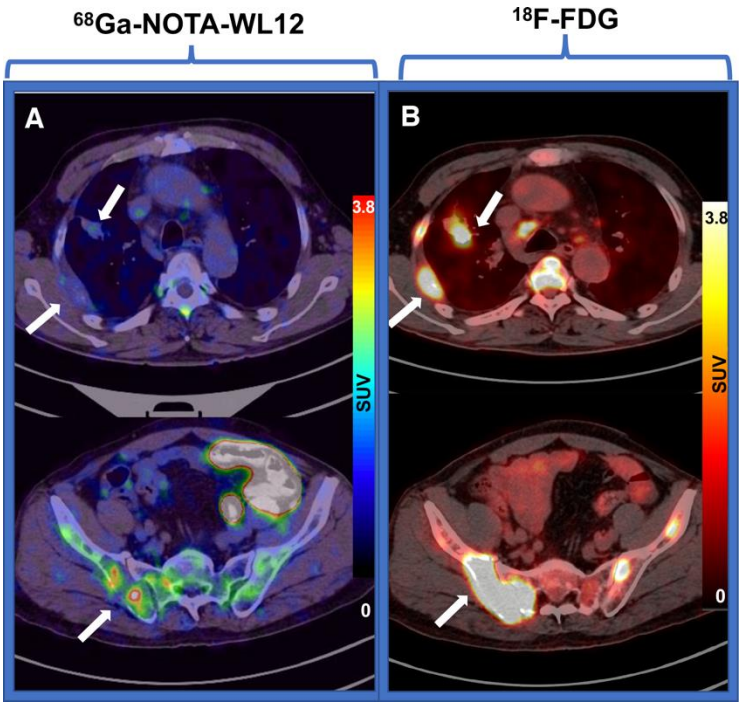

Figure 6. Patient 8, a 68-year-old man with lung adenocarcinoma, showed inhomogeneous intra-and-inter-tumoral uptake on [^{68}Ga]NOTA-WL12 PET/CT(A) and high homogeneous uptake in the tumors on FDG PET/CT (B).

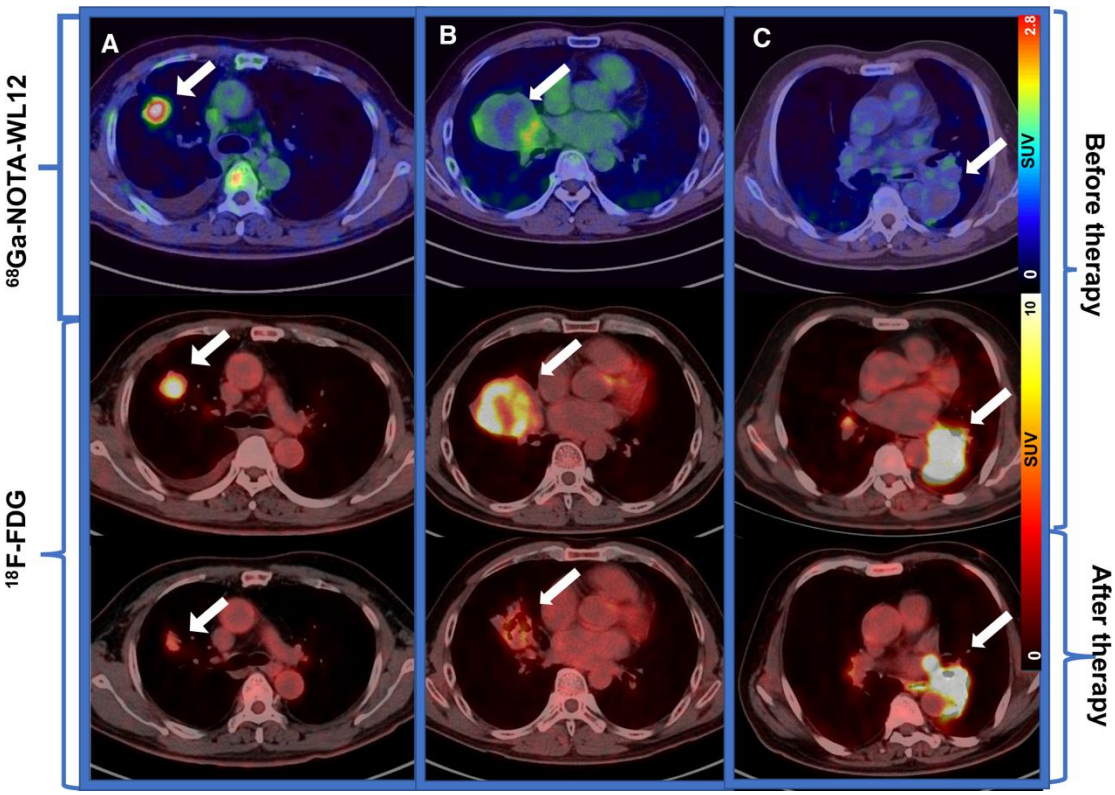

Figure 7. Patient 6, a 58-year-old man with adenocarcinoma and a PD-L1 TPS of 30%. The SUV_{max} of [^{68}Ga]NOTA-WL12 was 3.05 and that of FDG decreased from 8.03 to 3.10 (A). Patient 1, a 47-year-old man with squamous cell carcinoma and a TPS of 8%. The SUV_{max} of [^{68}Ga]NOTA-WL12 was 2.21 and that of FDG decreased from 9.13 to 3.54 (B). Patient 3, a 68-year-old man with squamous cell carcinoma and a TPS of 8%. The SUV_{max} of [^{68}Ga]NOTA-WL12 was1.84 and that of FDG increased from 16.55 to 21.38 (C).

Table 1. Patient Characteristics

Addition Of Wl12 (MG)	Patient No.	Sex	Age (Y)	Ecog Score	Tumor Type	PD-L1 Expression*	Clinical Stage	Tumor Size (Cm)	Therapy Regimen
0	1	M	47	1	LUSC	8%	cT4N2M1a IVa	7.2×6.1	Nab -Paclitaxel + Carboplatin + Pembrolizumab
0	2	M	72	0	LUSC	35%	cT2N3M0 IIIb	4×3.4	Paclitaxel + Cisplatin
5	3	M	68	0	LUSC	8%	cT4N1M1a IVa	5.8×4.7	Nab -Paclitaxel + Carboplatin + Pembrolizumab
60	4	M	68	1	LUAC	25%	cT4N1M0 IIIa	5.1×4.0	Nab-Paclitaxel + Carboplatin
	5	M	80	2	LUAC	40%	cT4N3M1c IVb	5.7×3.9	Toripalimab
	6	M	58	0	LUAC	30%	cT2aN2M1c IVb	3.1×2.3	Pemetrexed + Carboplatin + Pembrolizumab
120	7	M	63	1	LUSC	25%	cT2bN2M1b IVa	4.2×4.1	Pembrolizumab
	8	M	53	1	LUAC	35%	cT2bN2M1b IVa	3.1×1.9	Pemetrexed + Carboplatin + Sintilimab
	9	F	80	2	LUAC	80%	cT3N3M1c IVb	5.9×5.3	Pembrolizumab

*LUSC: lung squamous cell carcinoma; LUAC: lung adenocarcinoma.

Table 2. Organ observed doses and whole-body effective doses

Organ/Tissue	Absorved dose (mGy/MBq)
Adrenals	2.60e-02
Brain	8.80e-04
Esophagus	7.43e-03
Eyes	8.88e-04
Gallbladder Wall	3.21e-02
Left Colon	1.52e-02
Small Intestine	3.47e-01
Stomach Wall	8.41e-03
Right Colon	1.26e-02
Rectum	6.83e-03
Heart Wall	1.45e-02
Kidneys	3.42e-02
Liver	1.92e-01
Lungs	1.55e-02
Pancreas	2.13e-02
Prostate	4.39e-03
Salivary Glands	1.09e-03
Red Marrow	6.10e-03
Osteogenic Cells	4.05e-03
Spleen	2.89e-02
Testes	1.16e-03
Thymus	3.85e-03
Thyroid	2.15e-03
Urinary Bladder Wall	1.16e-02
Total Body	1.04e-02
Effective Dose (mSv/MBq)	1.85e-02

Graphical Abstract

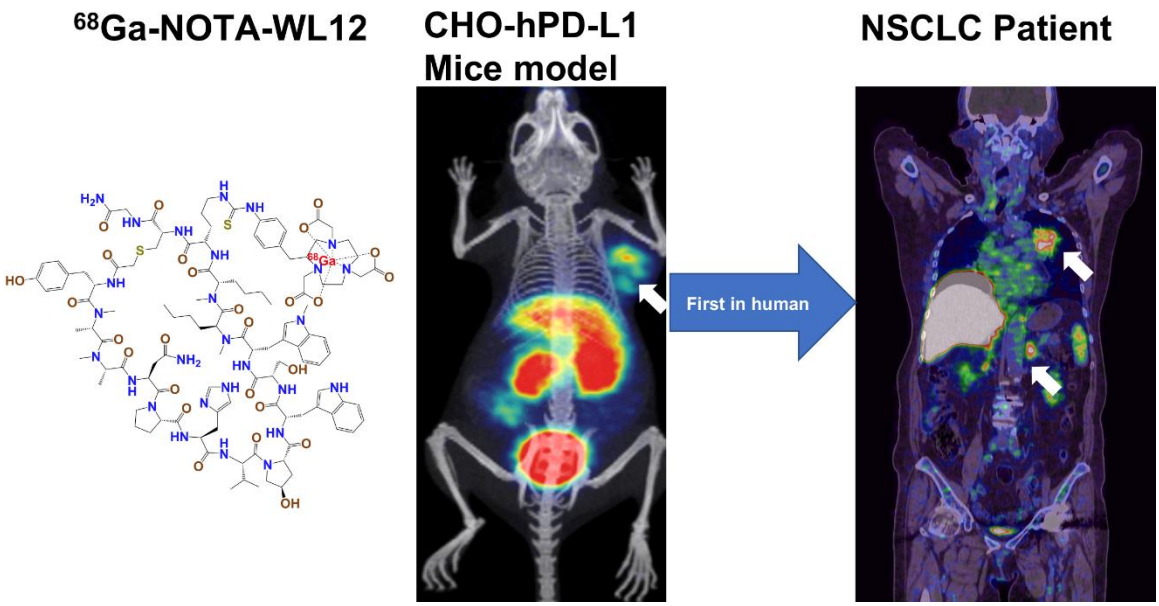

Supplemental information of "First-in-human evaluation of a PD-L1 binding peptide radiotracer in non-small cell lung cancer patients with PET"

SUPPLEMENTAL MATERIALS AND METHODS

Radiolabeling and Purification of ^{68}Ga-NOTA-WL12

NOTA-WL12 was obtained from Chinapeptides Company (Shanghai, China) as a custom service standard. ^{68}Ga was obtained from a ^{68}Ge/^{68}Ga radionuclide generator (ITG, Germany) and used to label the NOTA ligand. ^{68}Ga-NOTA-WL12 was synthesized by incubating $^{68}GaCl_3$ with the ligand in pH = 4.0 buffer at 60°C for 15 min. After Sep-Pak C18 (Waters, Germany) cartridge purification, the radiotracer was obtained by radio high-performance liquid chromatography (HPLC), and the radiochemical purification yield was 99% (Supplemental Figure 1). As shown in Supplemental Table 1, the ^{68}Ga-NOTA-WL12 solution complied with the Regulation of the Administration and Preparation of Positron Radiation Drugs by Medical Institutions. Radiopharmaceuticals are subjected to quality control analysis mainly to ensure their safety. The radiolabeled production of ^{68}Ga-NOTA-WL12 was typically 555-740 MBq with 30 μg of NOTA-WL12. The injection dose, ranging from 1.9-3.7 MBq/kg, was decided based on the patient's weight. Thus, the masses of the injected radiolabeled compounds injected differed, ranging from approximately 10-20 μg.

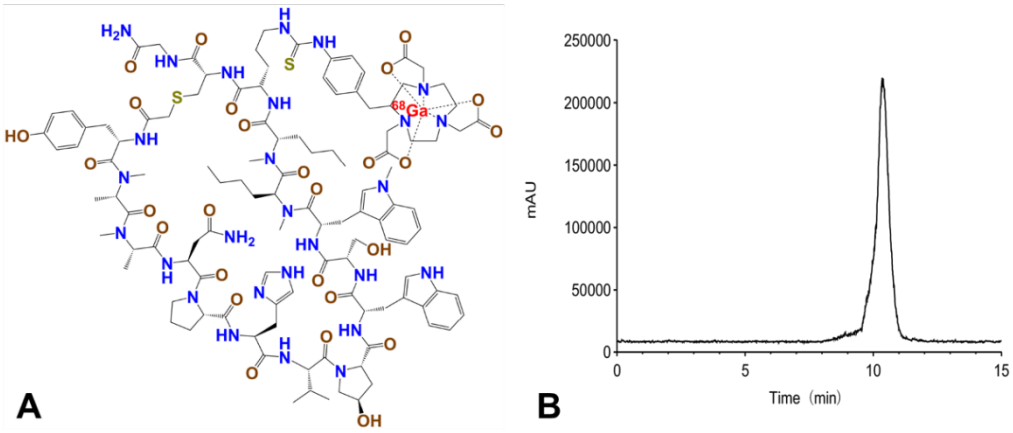

Supplemental Figure 1. Structure of ^{68}Ga-NOTA-WL12 (A). HPLC analysis of ^{68}Ga-NOTA-WL12 (B).

Supplemental Table 1. The quality control results of ^{68}Ga-NOTA-WL12

Parameter	QC Specification	QC Result
Appearance	Clear,colorless	pass
Volume	2.0-5.0mL	4.0 mL
pH	5.0-8.0	7.4
Radio-TLC	>95%	>99%
Radio-HPLC	>95%	>99%
Ethanol	<5%	<5%
Endotoxins	<15EU/mL	< 5EU/mL
Sterility	Sterile	Pass
Specific Activity	18.5- 296 GBq/μmol	74 GBq/μmol

The radiochemical purity was analyzed by radio HPLC (Supplemental Figure 1B), which was conducted on a C18 column (Zorbax 300SB-C18, 4.6×250 mm, 5 μm; Agilent, USA) with (A) H_2O (0.1% TFA) and (B) acetonitrile (0.1% TFA) using a linear A-B gradient from 95/5 (A/B) to 20/80 (A/B) over 15 min period with a flow rate of 1 mL/min and a UV wavelength of 220 nm. Radio TLC was conducted using iTLC-SG-Glass microfiber chromatography paper containing silica gel (Agilent Technologies, USA) on an AR 2000 system (Bioscan, USA). The pH of the injectate was measured by a pH meter (SP-2500, SUNTEX, China). The limulus test was performed to assay endotoxins. A direct inoculation method was employed to assess the sterility of the ^{68}Ga-NOTA-WL12 solution.

The in vitro stability test of ^{68}Ga-NOTA-WL12 was performed in saline and in 5% human serum albumin (HSA) at 37 ℃ at 30, 60 120 and 240 min. At different time points, 20 μL of the mixture was removed and used for the analysis of radiochemical purity by radio TLC (n=3). The radiochemical purity of the radiotracer in both solutions was over 95% after 240 min of incubation.

Radiotoxicity in mice

In the radiotoxicity study, fourteen BALB/c mice (16~19 g, female, 4~6 weeks old) were randomly divided into two groups. In the experimental group, each mouse was injected with 0.5 mL of ^{68}Ga-NOTA-WL12 at a dose of 1.57 GBq/kg (over 500-fold more than the dose used in

human subjects). In the control group, each mouse was injected with 0.5 mL of saline. At 1, 2, 3, 4, 5, 6 and 7 days postinjection, the mice were weighed, and routine blood tests were performed by the Animal Laboratory of Peking University Health Science Center.

Cell culture , flow cytometric analysis and cell uptake study.

CHO and CHO-hPD-L1 cells were cultured in F-12K medium supplemented with 10% fetal calf serum (Invitrogen; Thermo Fisher Scientific, Inc.) and 1% penicillin/streptomycin (Invitrogen; Thermo Fisher Scientific, Inc.) at 37°C in a humidified incubator containing 5% CO_2. The CHO and CHO-hPD-L1 cell lines were subjected to flow cytometric analysis. Single CHO and CHO-hPD-L1 cell suspensions were stained with PE-conjugated anti-human CD274 (PDL1) (329705, BioLegend) at a final concentration of 1 μg/ml for 30 min at 4°C in the dark. Subsequently, dead cells were eliminated by adding 1 μg/ml propidium iodide (PI) for 10 min at room temperature. Flow cytometry analyses were performed on a BD FACSCalibur™ instrument (BD Biosciences). Data were analyzed with Flow Jo software (version 10.6.2).

CHO-hPD-l1 and CHO cells were plated on 24-well cell plates (1×10^6 cells per well) 24 hours before the study. Half a milliliter of fresh medium containing 1 μCi of the radiotracer was added to each well, and the cells were cultured in an incubator at 37 ℃ with 5% CO_2. After incubation for 5, 30, 60 and 120 min, the medium was removed, and cells in each well were then washed 2 times with 1 mL of cold phosphate-buffered saline (PBS) and lysed with cold NaOH (1 *M*). In the blocking study, cells in each well were co-incubated with 20 μg of the WL12 peptide.

The radioactivity of cells in each well was measured with a γ-counter, and the results are shown as the percentage of the added dose (% AD) / 10^6 cells.

Flow cytometric analysis and small-animal PET imaging

Small-animal PET Imaging

NOD/SCID mice bearing CHO-hPD-L1 tumors and CHO tumors were intravenously injected with ~7.4 MBq (~0.17μg) of ^{68}Ga-NOTA-WL12 in 200 μL of saline. The mice were anesthetized with 3% isoflurane before the micro-PET scan, and 1.5% isoflurane was maintained during the scanning. Fifteen-minute static micro-PET imaging was performed at 0.5, 1 and 2 h after injection. In the blocking study, the mice were coinjected with 50 μg of unlabeled WL12. Fifteen-minute static micro-PET scans were then acquired at 1 and 2 h after injection. Imaging was performed on a Super Nova PET scanner using an 80-mm-diameter transaxial field of view, and ordered-subset expectation maximization 3-dimensional reconstruction algorithms with attenuation and random corrections were performed. The final images were displayed by Avatar3.lnk workstation software. In the PET/CT imaging analysis, the region of standardized uptake value (SUV) was calculated. To further confirm the PD-L1 expression level in tumor cells, PD-L1 immunohistochemistry was conducted on CHO-hPD-L1 tumors and CHO tumors.

Radiation Dosimetry Calculations.

Methods for dosimetry analysis.

The heart, lung, liver, spleen, pancreas, kidneys, uterus, urinary bladder and remainder of the body were selected as source organs. The volume of organs was determined manually by making an outline of the organ on CT imaging layer by layer. Whole-organ activity (MBq) was calculated by multiplying organ volume by mean counts/mL and dividing by 1000. The percentage of injected activity was calculated to generate the activity concentration-time curve of each source organ with no consideration of the biological half-life. Time-integrated activity coefficients were calculated individually, biexponential curve fitting was applied to activity concentration-time curves of the uterus and urinary bladder content, while mono-exponential curve fitting was applied to other source organs, to calculate the areas under the curve, and human organ dosimetry was further estimated using OLINDA/EXM software (version 2.0; Hermes Medical Solutions AB). Organ-absorbed doses and total effective doses, as well as residence time for each patient, were obtained using reference adult male and female models.

Supplemental Imaging analysis.

The comparison of coefficients of variation between SUV/L_{mean} and ratio of tumor to background at 1h and 2h (Supplemental Figure 2).

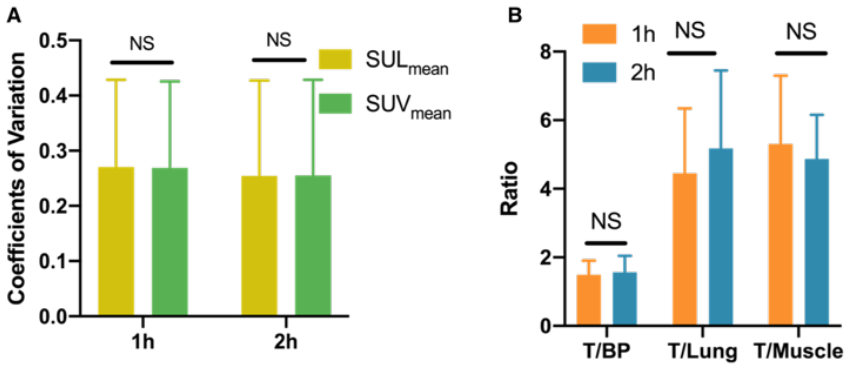

Supplemental Figure. 2 The coefficient of variations of organs in 1 and 2 h made no differences between SUL_{mean} and SUV_{mean} (A). The ratios of tumor to background (blood pool, lungs, and muscle), as T/BP, T/Lung and T/Muscle, were not significantly different at 1 h and 2 h (B). NS, no significant differences.

Supplemental Imaging analysis.

Supplemental Table. 2 Comparison of Coefficients of Variation between SULmean and SUVmean at 1 and 2 h after injection

	1 h		2 h	
	SUL_{mean}	SUV_{mean}	SUL_{mean}	SUV_{mean}
Heart	0.15772569	0.16017626	0.1283289	0.12699374
Blood Pool	0.24965731	0.24769874	0.28701308	0.29322299
Lung	0.28079196	0.27352511	0.22403846	0.2322501
Liver	0.19453637	0.18744827	0.08292365	0.08019268
Spleen	0.18443101	0.18718625	0.1596635	0.16388395
Muscle	0.134009	0.13312701	0.16478173	0.16248077
Bone Marrow	0.22410873	0.22777378	0.330907	0.32710491
Small Intestine	0.63201945	0.62745836	0.62348588	0.62479503
Tumor	0.32675577	0.32793333	0.31942288	0.32345226

Supplemental Imaging analysis.

Uptake measurements of normal organs (Supplemental Figure 3).

The uptake of some normal organs was measured by multi-sites to make a more precise result for comparison. The blood pool was measured in the right ventricle, ascending aorta and descending aorta(totally 3 sites). The liver was measured in segments II-VIII (7 sites in total). The spleen was measured at superior, inferior, left, right and central positions (a total of 5 sites). Each kidney was measured at superior, central and inferior positions (a total of 6 sites). And the Small intestine was measured in upper, middle and lower abdomen(totally 3 sites). And the specific sites of the organs were depicted as follows.

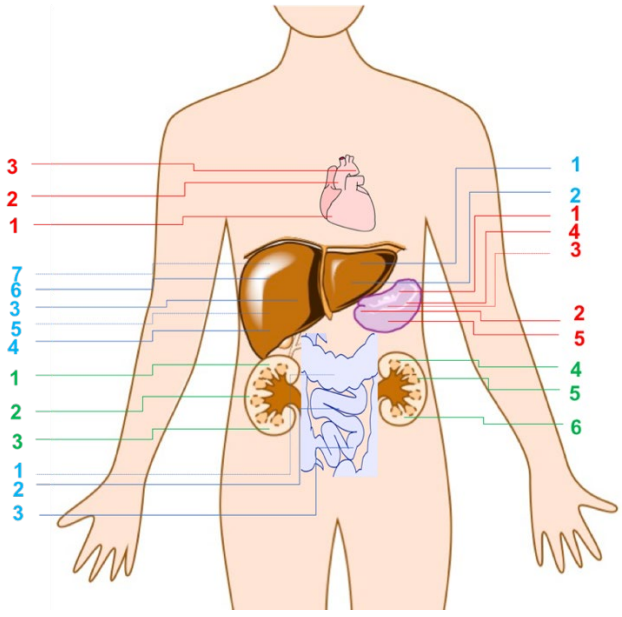

Supplemental Figure 3. Uptake measurements of normal organs

SUPPLEMENTAL RESULTS

Radiotoxicity in mice

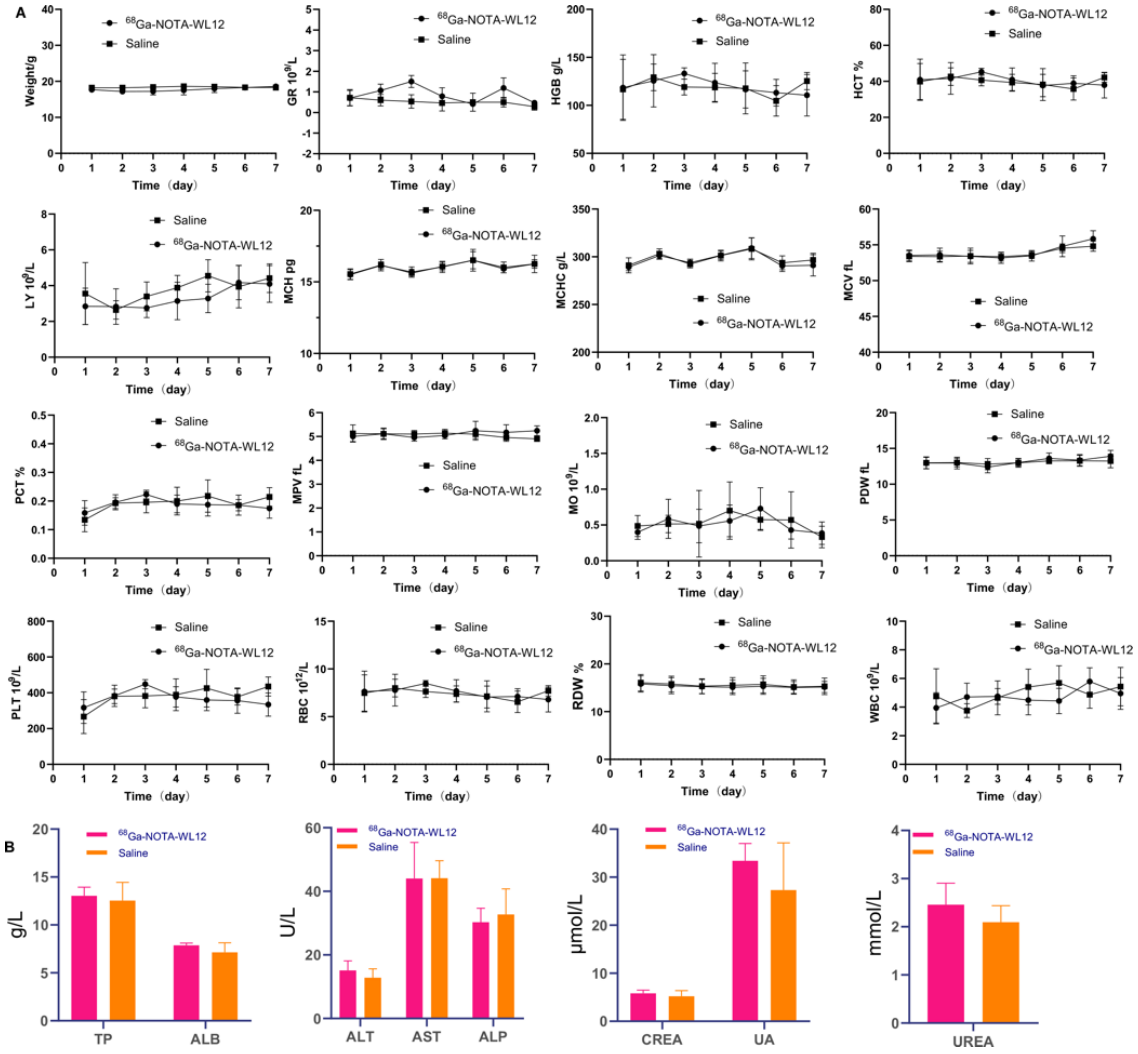

Supplemental Figure 4 (A): The results of weight and routine blood test of mice in radiotoxicity study of ^{68}Ga-NOTA-WL12 (n=7). GR (neutrophil), HGB(hemoglobin), HCT (hematocrit) , LY (absolute value of lymphocytes), MCH (mean corpuscular hemoglobin), MCHC (mean corpuscular hemoglobin concentration), MCV (mean corpuscular volume) , PCT (platelet counts), MPV (mean platelet volume), MO (absolute value of monocyte), PDW (platelet distribution width), PLT (platelet counts), RBC (red blood cell count), RDW(red blood cell distribution width), WBC

(white blood count). (B): The results of biochemical tests. TP (total protein), ALB (albumin), ALT (alanine aminotransferase), AST (aspartate amino transferase), ALP (alkaline phosphatase), CREA (creatinine)，UA (Uric Acid), UREA (carbamide).

In Vitro Cellular Studies and Small-Animal PET Imaging.

Uptake of ^{68}Ga-NOTA-WL12 of different cell lines in vitro and in vivo (Supplemental Figure 5).

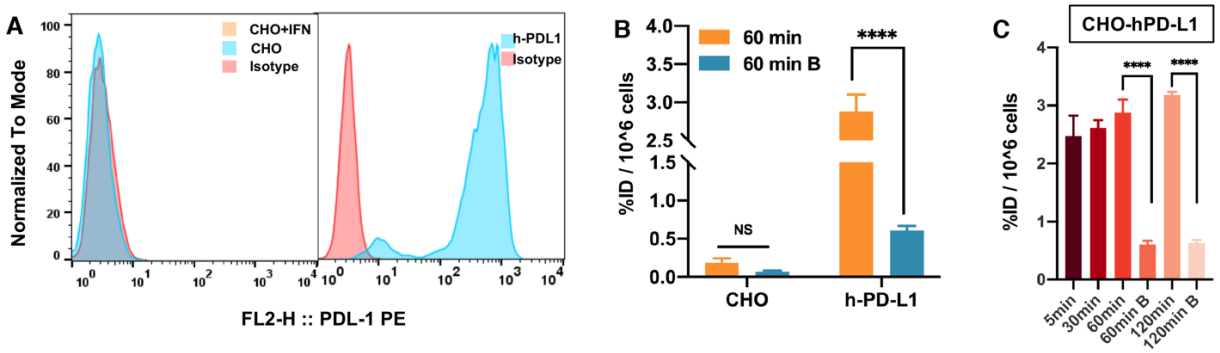

Supplemental Figure. 5 Flow cytometric analysis of CHO and CHO-hPD-L1. (A). In vitro uptake of ^{68}Ga-NOTA-WL12 of CHO and CHO-hPD-L1 at 60 and 120 min (B). Cell uptake of ^{68}Ga-NOTA-WL12 without and with a blocking dose in CHO-hPD-L1 cell lines (C).

In Vitro Cellular Studies and Small-Animal PET Imaging.

^{68}Ga-NOTA-WL12 uptake in negative control CHO tumor model by small-animal PET imaging (Supplemental Figure 6A). Immunohistochemistry analysis of PD-L1 expression in CHO-hPD-L1 tumors(Supplemental Figure 6B).

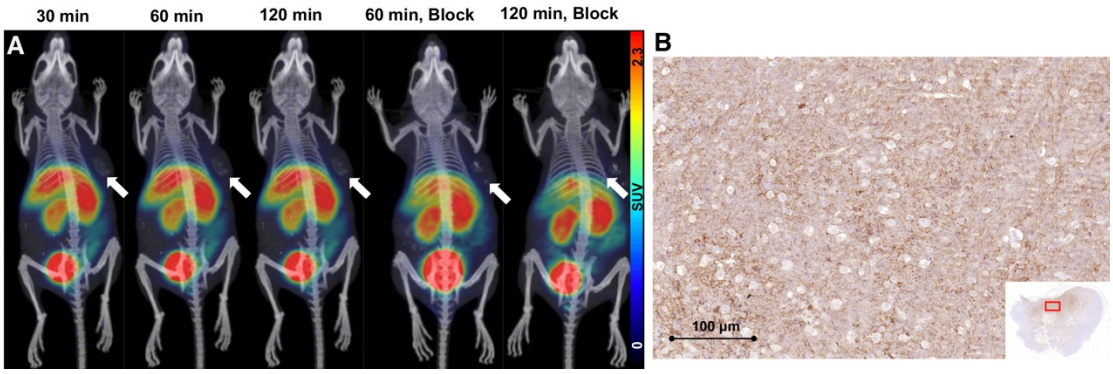

Supplemental Figure. 6 A, ^{68}Ga-NOTA-WL12 PET/CT imaging without and with blocking dose in NOD/SCID mice bearing CHO tumors at different time points. B, Immunohistochemistry analysis of PD-L1 expression in CHO-hPD-L1 tumors (100 µm).

Biodistribution in NSCLC patients.

The comparison of radioactivity and percentage of injection (Supplemental Figure 7)

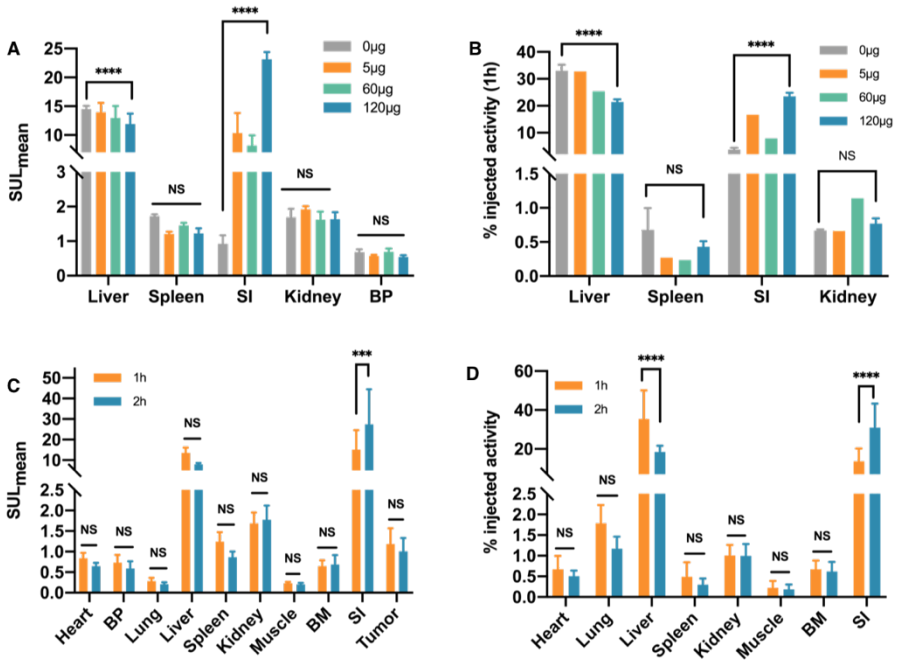

Supplemental Figure 7. SUL_{mean} of liver, spleen, small intestine (SI), kidney and blood pool (BP) given different doses of WL12(0, 5, 60 and 120 μg) at 1h after injection (A). Percentage of injection of high-uptake normal organs given different doses of WL12 (B). Comparison of SUL_{mean} of normal organs and tumors at 1and 2 h (C). Comparison for percentage of injection of normal organs at 1and 2 h (D).

Tumor uptake and correlation with immunohistochemistry

The relationship between tumor uptake(^{68}Ga-NOTA-WL12 and ^{18}F-FDG) and TPS of PD-L1 immunohistochemistry (IHC) expression (Supplemental Table 2).

Supplemental Table 3. Relationship of tumor radioactivity uptake with PD-L1 IHC.

	^{68}Ga-NOTA-WL12		^{18}F-FDG	
	R_s *	*P**	R_s	*P*
SUV_{max}	0.86	0.0029	0.576	0.1046
SUL_{max}	0.7643	0.0165	0.4541	0.2195
SUV_{peak}	0.9349	0.0002	0.5529	0.1226
SUL_{peak}	0.8469	0.004	0.4261	0.2528
SUV_{mean}	0.867	0.0025	0.6937	0.0382
SUL_{mean}	0.7723	0.0147	0.5864	0.097
T/BP (SUV)[#]	0.5313	0.141	0.3491	0.3571
T/BP (SUL) [#]	0.7479	0.0205	0.3384	0.3731

*: R_s, square of correlation coefficient from Spearman correlation; *P*: value for significance; #: ratio of tumor SUV/L_{max} to blood-pool SUV/$L_{mean.}$ IHC, immunohistochemistry.

Relationship of ^{68}Ga-NOTA-WL12 uptake and therapy evaluation.

Tumor radio-uptake and therapy evaluation (Supplemental Table 4).

Supplemental Table 4. Tumor radioactivity uptake and therapy evaluation

Patient No.	PD-L1 TPS	$SUV_{max,}$ WL12	$SUV_{max,}$ FDG		PERCIST	RECIST
		Before Therapy	Before Therapy	After Therapy		
1	8%	2.21	9.13	3.54	PMR	SD
3	8%	1.84	16.55	21.38	PD	PD
6	30%	3.05	8.03	3.1	PMR	SD

Partial metabolic response (PMR); Stable disease (SD); Progressive disease (PD).

1. Chatterjee S, Lesniak WG, Gabrielson M, et al. A humanized antibody for imaging immune checkpoint ligand PD-L1 expression in tumors. *Oncotarget.* 2016;7:10215-10227.